Density Functional Theory in Prediction of Four Stepwise Protonation Constants for Nitrilotripropanoic Acid (NTPA)

Krishna K. Govender and Ignacy Cukrowski*

Department of Chemistry, Faculty of Natural Sciences, University of Pretoria, Lynnwood Road, Hillcrest, Pretoria 0002, South Africa

Received: December 15, 2008; Revised Manuscript Received: February 4, 2009

It has been demonstrated for the first time that prediction of several consecutive protonation constants for the highly and negatively charged molecules, such as nitrilotripropanoic acid (NTPA), is possible with acceptable accuracy when isodesmic reaction (IRn) methodology, instead of commonly employed thermodynamic cycle (TC), is employed. Four stepwise protonation constants of NTPA were computed (RB3LYP/6-311+G(d,p) level of theory employing PCM/UA0 solvation model) to within ±1 log unit of experimental data with an average error in the protonation constant of about 0.5 log unit. This good agreement was achieved for minimum energy structures of NTPA (studied ligand) and iminodiacetic acid (reference molecule). Results obtained strongly support the view that full conformational analysis should be seen as prerequisite for computing protonation/dissociation constants from IRn and possibly also from TC. Methodology proposed here broadens up, in our opinion, a scope of studying protonation constants computationally and opens up a new field of applications for poly charged ligands. TC did not work here at all as proton on N-atom was not preserved in gas-optimized structures; this proton always protonated available COO^- group instead.

1. Introduction

The protonation/dissociation property of a compound is very important in chemistry, biology, and material sciences, because the ability of a compound to donate or accept a proton is fundamental to understanding many chemical and biochemical processes.[1,2] An example in medicinal chemistry is the ability of drugs to pass biological membranes as well as their potential to interact with intracellular receptors, both of which are affected by the readiness of the drug to accept or donate a proton.[3] Availability of dissociation (protonation constants as well as complex formation constants) is of fundamental significance as it allows for modeling of solution composition at required experimental conditions, such as blood plasma, natural waters, industrial effluents, etc. Experimental techniques provide protonation/dissociation constants typically with uncertainty on the second decimal place of the log unit and well-renown compilations, such as by Martell and Smith[4] or IUPAC[5] are readily availably.

However, there is an intrinsic interest to develop theoretical procedures that would eventually match experimental accuracy. This is not only because not all chemical species are readily amenable or available (due to small quantity available) to experimental characterization but also due to fundamental insight gained during theoretical modeling as well as prediction (or evaluation) of thermodynamic parameters related to the compound and reaction(s) in which this compound is involved. There have been a number of studies performed thus far where dissociation constants were predicted theoretically with considerable accuracy.[1−3,6−50] Dissociation constants were studied for molecules of carboxylic acids,[1−3,6−21] amides,[22,23] bicarbonates,[16,24] and proteins,[25] among others. However, it is important to emphasize that the molecules studied thus far were predominantly neutral or singly charged and on average the reported computed dissociation constants are within ±1.0 log unit when compared with experimental values. From the theoretical point of view, this might be regarded as an excellent result particularly because the deviation in computed value by a log unit is equivalent to the accuracy of energy computed in the range of a single kilocalorie per mole. Unfortunately, a large drop in accuracy of computed dissociation constants is observed when multiple and particularly negative charges on a molecule are present;[51] hence there is very little published on stepwise multiple-dissociation constants in solvent (water).[24]

To the best of our knowledge, all the reported theoretical values are from thermodynamic cycles that typically involve two-step operation, namely, (i) full gas-phase energy optimizations of components involved in dissociation reaction, followed by (ii) single point calculations in solvent (water) on those structures from which ΔG(aq) is obtained and used to calculate the dissociation constant at room temperature. Four thermodynamic cycles were recently evaluated by Liptak and Shields[11] on several singly dissociable simple carboxylic acids using complete basis set and Gaussian-*n* models combined with Barone and Cossi's implementation of CPCM.[52] The high-level ab initio CBS-QB3[53] and CBS-APNO[54,55] methods (using HF 6-31 G(d) and HF 6-31+ G(d)) with CPCM generated smallest inaccuracy of about 0.5 log unit when commonly used, and the simplest thermodynamic cycle (without involving water molecule) was employed.[11] Similar accuracy was reported by Namazian et al.[9] recently who used CPCM solvation energies at the B3LYP/6-31+G(d) level in conjunction with CBS-QB3 or G3 gas-phase energies of trifluoroacetic acid and its anion. It appears that there is a strong tendency to avoid water and simple proton in thermodynamic cycle computations and rather use most recent experimental values of −6.28 kcal/mol[12,56] and −265.9 kcal/mol[16] or −263.98 kcal/mol[16] for the gas-phase Gibbs free energy of H^+ and solvation energy of H^+ in water, respectively.

A somewhat more elaborate approach was also tested[6,7] where the thermodynamic cycle was combined with an isodesmic

* E-mail: ignacy.cukrowski@up.ac.za.

10.1021/jp811044b CCC: $40.75 © 2009 American Chemical Society
Published on Web 03/23/2009

reaction involving acetic acid (and its dissociation reaction) as a single reference molecule used to theoretically predict numerous dissociation constants of monodissociable organic acids; the differences between experimental and theoretical values were between a fraction of and up to about 5 log units for some molecules. A new model of dissociation constant computation, called S03 and based on thermodynamic cycle, was proposed by Barone et al.[2] who used PBE0/6-31+G(d,p) and PBE0/6-311+G(2d,2p) level of theories for full energy optimization and single point calculations in the gas phase, respectively, as an initial step from which gas-phase basicities of eight investigated organic acids were predicted. This was followed by estimation of solvation Gibbs energies by single point HF/6-31+G(d,p) calculations using geometries optimized in water at the PBE0/6-31+G(d,p) level. Although gas-phase basicities were of analytical accuracy, the dissociation constants in water were of commonly reported differences of ±0.7 log units from experimental values with aqueous solution geometries; much worse results were obtained with gas-phase geometries used for single point calculations in solvent.

We embarked recently on the DFT-based theoretical studies of metal complexes[57] to explore physical and molecular (and structural) properties controlling the strengths of complexes formed. Our particular interest is to understand why "small" but apparently significant structural changes in a ligand are causing "'unexpected" large changes in stability constants of metal complexes; it is of great importance and significance to find out about fundamental rules governing the strength of metal−ligand interactions on atomic and molecular level. One such, among many known examples, set of ligands is nitrilotriacetic acid (NTA) and nitrilotripropanoic acid (NTPA) whose structural difference is an additional $-CH_2-$ group in each acid-containing arm of the ligand NTPA. Even though the kind and the number of donor atoms, which form bonds with a metal ion, is the same for the both ligands the formation constants of metal complexes with NTA (strong complexing agent) are several log units larger when compared with equivalent complexes involving NTPA[4] (weak complexing agent). To illustrate this point, the complex ML of Cd(II) with NTA is over 6 orders of magnitude more stable when compared with NTPA ($\log K_1 = 9.76$ and 3.4, respectively). The difference must be even larger for Pb(II) ($\log K_1 = 11.48$ for NTA) as there is no value reported for NTPA,[4] it appears that the Pb−NTPA complex must be very weak and hence difficult to study experimentally.

The first obvious step necessary to achieve our ultimate goal is to determine theoretically the stepwise protonation constants of the ligands of interest. This must be seen as a challenge on its own as (i) there were no successful reports yet where ligands with three negative charges were investigated and (ii) results reported for less negatively charged ligands were significantly different when compared with experimental data. We examine here the applicability of thermodynamic cycles and carefully designed isodesmic reactions for theoretical prediction of four stepwise protonation constants of the ligand NTPA. This work demonstrates that, at least in the case of negatively and multiply charged ligands, the best option in theoretical prediction of protonation (dissociation) constants is the isodesmic reaction; theoretically predicted protonation constants for NTPA ligand reported in this work compare well with experimental values.

2. Computational Details

All computational calculations were performed with the aid of Gaussian 03 software package.[58] Gas-phase and solvent (water, $\varepsilon = 78.39$) geometry optimization of protonated NTPA forms was performed at the RB3LYP/6-311+G(d,p) level of theory.[59] As it was pointed out previously,[24] it is essential and of paramount importance to include diffuse functions for anions. The full optimization in solvent involved the default solvation model, i.e., Tomasi's polarized continuum model (PCM),[60−62] and UA0 radii (united atom topological model). With this model the cavity is defined as the union of a series of interlocking atomic spheres. The effect of polarization of the solvent continuum is represented numerically and it is computed by numerical integration.[63] Single point calculations (SPCs) in solvent were carried out at the same level of theory (i) on the gas-optimized structures using PCM-UA0 model and (ii) on solvent optimized structures using the polarizable conductor model (CPCM)[52,64] and UAHF radii (united atom for Hartree−Fock). With this model the solute cavities are modeled on the optimized molecular shape and include both electrostatic and nonelectrostatic contributions to energies.[12]

Geometry optimization of all NTA and iminodiacetic acid (IDA) protonated forms (used as reference molecules in isodesmic reactions) was carried out in solvent using the same procedure as for NTPA; there was no need to perform a single point calculation. Frequency calculations were also performed, along with the geometry optimization, to ensure that each of the optimized molecules was in fact at a minimum energy (for all structures considered in this study the imaginary frequencies were not present).

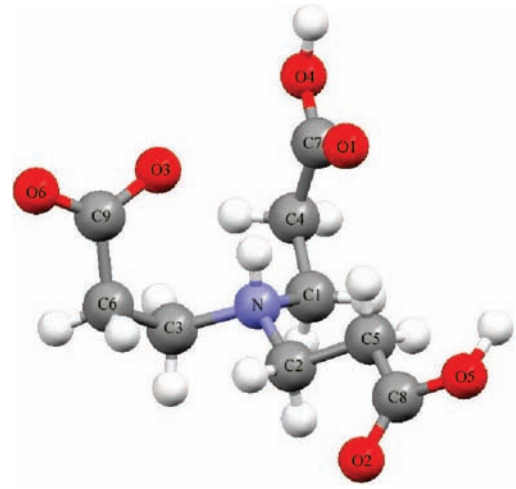

Figure 1. Fully labeled reported crystal structure of the H_3L form of NTPA.

3. Results and Discussion

Level of Theory. From literature reports it follows that there is no strong evidence in support of using high level theories instead of commonly applied cheaper (time and hardware) B3LYP, for instance. Our approach implemented here, to validate computational methods, was to select a combination of level of theory and basis set in such a way that it would reproduce a crystallographic structure with commonly acceptable in the field accuracy. Fortunately, there are available two crystallographic H_3L structures of the ligand NTPA;[65−66] the fully labeled reported crystal structure is shown in Figure 1. It is important to note that the N-atom is protonated (^+H-N) in the solid state form of H_3L ligand (NTPA), leaving one carboxylic group being deprotonated ($-COO^-$); hence this molecule is overall neutral, but with two local, positive and negative, charges. The energy-optimized solvent crystallographic structure is marked further as H_3L^*. We used H_3L^* to generate

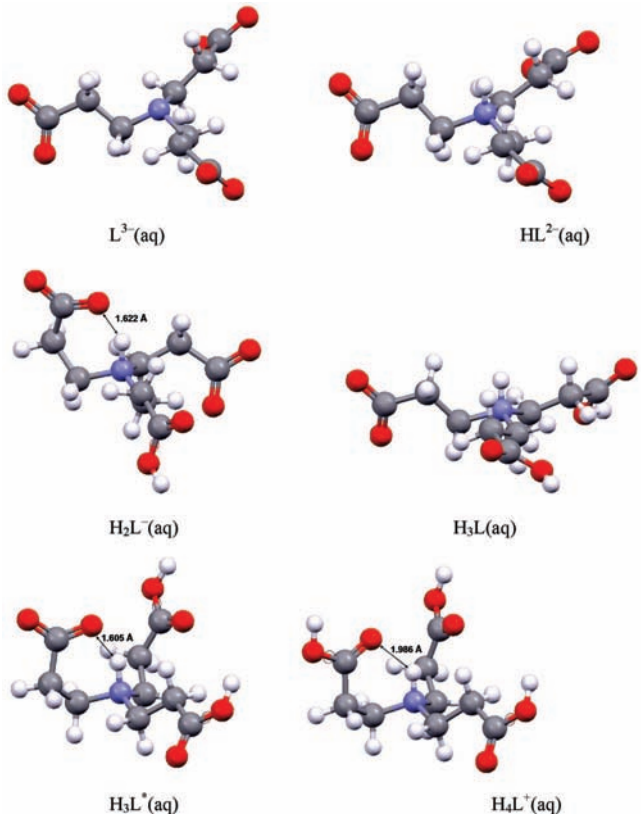

Figure 2. Structures of all protonated forms of the NTPA ligand fully optimized at the RB3LYP/6-311+G(d,p) level of theory in solvent (PCM/UA0).

input structures of the remaining four possible protonated forms of NTPA, namely, H_2L^-, HL^{2-}, L^{3-} (fully deprotonated ligand), and H_4L^+ (fully protonated form of the ligand). Starting from H_3L*, input structures for full energy optimization of H_2L^- (by removing a dissociable proton from the −COOH group) and H_4L^+ (by simply adding a proton to O-atom) were generated.

A similar procedure was followed to computationally generate HL^{2-} and L^{3-}, where a proton was removed from energy optimized structure to generate the product of stepwise dissociation reaction. Due to the reasons discussed in detail further in the text, we also constructed H_3L that was structurally different when compared with H_3L*. The computed structural matrix of solvent-optimized H_3L* and H_3L together with the data available from the Cambridge Structural Database (CSD)[66] is given in Table S1, Supporting Information. It is seen that the energy-optimized solvent structure (H_3L* in Figure 2), when the input was that of the reported H_3L crystallographic structure, can be regarded as fully satisfactory (Table S1, Supporting Information; dihedral angles were not compared because they must vary in different protonated forms of NTPA). The bond lengths and angles were reproduced to within -0.010 ± 0.013 Å and $-0.94 \pm 2.25°$, respectively; the difference (Δ) means experimental minus computed value. On average, the computed values are slightly overestimated and this is most likely due to energy optimization of a single molecule with ignoring lattice effects. More rewarding is the fact that the energy minimized H_3L molecule has marginally smaller differences when compared with crystallographic data; the bond lengths and angles were reproduced to within -0.012 ± 0.012 Å and $-0.62 \pm 1.92°$, respectively, and the differences between the two optimized structures (δ = H_3L* − H_3L) we consider as negligible, -0.002 ± 0.010 Å (bonds) and $-0.32 \pm 1.29°$ (angles). This gave us confidence that all constructed structures should be seen as sufficiently reliable for further theoretical considerations. Also, data seen in Table S1 (Supporting Information) show that the RB3LYP/6-311+G(d,p) level of theory in conjunction with PCM/UA0 solvation model can be regarded as sufficient for the purpose of our studies.

All protonated forms of the NTPA ligand that were energy-optimized in solvent, including the crystal structure H_3L*, are shown in Figure 2. It is seen that H_2L^-, H_3L*, and H_4L^+ have strong H-bonds, C−O$^-$···H−N, and their lengths are 1.622, 1.605, and 1.986 Å, respectively, whereas H_3L is a symmetrical molecule (without any evidence of intramolecular bonding) that resembles to a large extent structures of L^{3-} and HL^{2-}.

Thermodynamic Cycle. In the field of metal−ligand equilibria studies, the complex formation constants and protonation (K_H) instead of dissociation (K_a) constants are used in solving the mass-balance equation needed to develop the most likely metal−ligand model (complexes formed) and refine stability constants of all metal-containing species. There are several important compilations of ligand protonation and complex formation constants, among them by Martell and Smith[4] and very recent one by IUPAC.[5] NTPA has four protonation constants

$$L^{3-} + H^+ \leftrightarrow HL^{2-} \qquad K_H^{(1)} = \frac{[HL^{2-}]}{[L^{3-}][H^+]} \tag{1}$$

$$\vdots \qquad\qquad \vdots$$

$$H_3L + H^+ \leftrightarrow H_4L^+ \qquad K_H^{(4)} = \frac{[H_4L^+]}{[H_3L][H^+]} \tag{2}$$

and the values at several ionic strengths (μ) and temperatures are known from experiment.[4,5] The thermodynamic cycle (TC) was utilized in the literature mainly to theoretically estimate dissociation constants that in the case of NTPA can be written as

$$H_4L^+ \leftrightarrow H_3L + H^+ \qquad K_a^{(1)} = \frac{[H_3L][H^+]}{[H_4L^+]} \tag{3}$$

$$\vdots \qquad\qquad \vdots$$

$$HL^{2-} \leftrightarrow L^{3-} + H^+ \qquad K_a^{(4)} = \frac{[L^{3-}][H^+]}{[HL^{2-}]} \tag{4}$$

In eqs 1−4 concentrations are used instead of activities because most of experiments are performed at selected ionic strength and temperature, according to envisaged practical application, such as, for instance blood plasma modeling that would require data at μ = 0.15 mol L^{-1} (Na^+(aq),Cl^-(aq)) and 37 °C. The computed value of ΔG(aq) can be used to calculate the nth stepwise dissociation constant at 25 °C that, for convenience, is commonly reported as a pK_a value. The protonation reaction is the reverse of the weak acid dissociation reaction, and in the case of stepwise reactions the following equation holds

$$\log K_H^{(k)} = \log \frac{1}{K_a^{(n)}} = pK_a^{(n)} \tag{5}$$

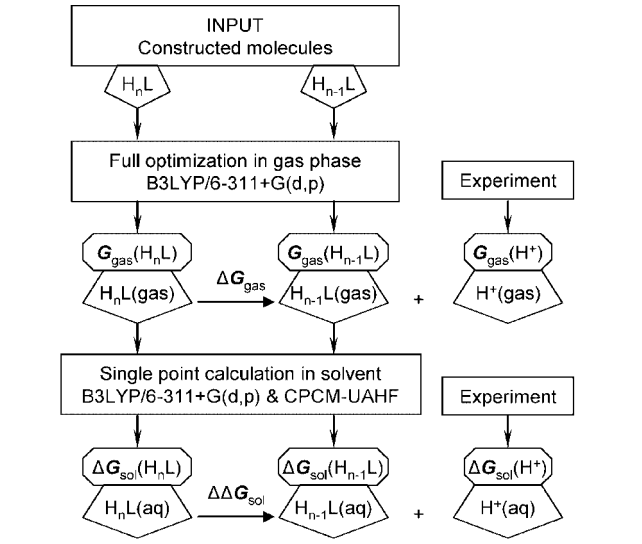

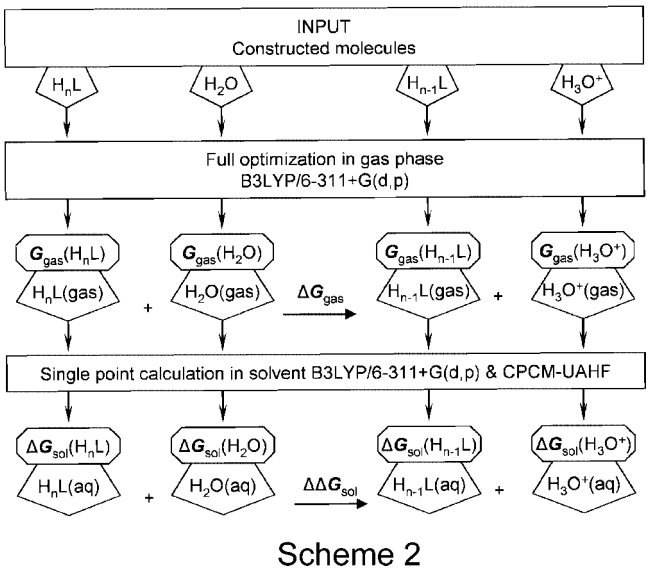

Figure 3. TCs employed in this work.

where $k = 1 + m - n$, m standing for the highest dissociation constant (here $m = 4$). Note that the ligand NTPA has three acidic groups and only three dissociation constants would be reported, and hence, the dissociation reaction (eq 3) most likely would not be considered as the first dissociation reaction, log $K_a^{(1)}$, in theoretical prediction of pK_a values employing TC-based methodology. However, due to the protonation/deprotonation of the N-atom in NTPA, one must consider also the first protonation constant, log $K_H^{(1)}$, as described by the protonation reaction (eq 1). From this follows that the fourth dissociation constant of NTPA is linked through eq 5 with the first protonation constant of this ligand. n indicates an nth consecutive dissociation constant, $1 \le n \le m$, and k applies to a kth consecutive protonation constant, $1 \le k \le m$. The above is well-known in the field of metal−ligand equilibria studies, but it is provided here for convenience and to ensure clarity in the nomenclature used.

Two TCs were considered in this work, and they are shown in self-explanatory fashion in Figure 3 as Scheme 1 and 2 (charges on the ligand species are omitted for simplicity throughout the text). To apply TC, one needs to optimize each of the protonated form of the ligand NTPA in the gas phase first. It is important to stress here that the moment solid NTPA is placed in water (the H_3L reagent has three protons present on carboxylic groups), the N-atom is protonated instantly and at least one proton on the propanoic acid arm dissociates fully. The problem experienced here during energy optimization in the gas phase of the crystallographic H_3L input structure that contains the protonated nitrogen atom (as it is present in a solution) was that this proton shifted to the COO^- group to form −COOH. Numerous input structures were tested, but each time the presence of hydrogen on N-donor atom was not preserved. This phenomenon was also reported in the literature for the ligand aspartic acid.[21,67] In attempt to preserve the H-atom on nitrogen, another conformer of H_3L was built with all carboxylic groups placed as far as possible from the central N-atom (H_3L seen in Figure 2). Unfortunately, even in this case energy optimization in the gas phase has also resulted in deprotonation of the N-atom and formation of −COOH with H-atom involved in a O−H···N hydrogen bond.

Clearly, in the gas phase the molecule H_3L does not exist in zwitterionic form. Because of that, TC could not be applied to the H_3L and H_4L forms of NTPA and we had to restrict our theoretical studies only to the first two protonation reactions from which HL and H_2L are formed. The values of G_{gas} and ΔG_{sol} are shown in Table 1 together with minimum energies after zero-point vibrational energy (ZPVE) corrections, E_{min}, of optimized molecules. The values of ΔG_{gas}, $\Delta\Delta G_{sol}$, and ΔG_{aq} were calculated using well-known relationships (eqs 6−8)

$$\Delta G_{gas} = \sum G_{gas}(\text{products}) - \sum G_{gas}(\text{reactants}) \quad (6)$$

$$\Delta\Delta G_{sol} = \sum \Delta G_{sol}(\text{products}) - \sum \Delta G_{sol}(\text{reactants}) \quad (7)$$

$$\Delta G_{aq} = \Delta G_{gas} + \Delta\Delta G_{sol} \quad (8)$$

and dissociation constants $K_a^{(n)}$ were obtained from eqs 9 and 10[11,68] in case of TC 1 and TC 2, respectively.

$$\Delta G_{aq}^{(n)} = -RT \ln K_a^{(n)} \quad (9)$$

$$\Delta G_{aq}^{(n)} - RT \ln[H_2O] = -RT \ln K_a^{(n)} \quad (10)$$

As shown in Figure 3, Scheme 1, in the case of the proton ion, the experimental values of −6.28 and −264.61 kcal/mol for G_{gas} and ΔG_{sol} were used, respectively.[12,32] Also, in final calculations of dissociation constants, appropriate correction of −1.89 kcal mol^{-1} (corresponding to the free energy change accompanied by the reversible state change of 1 mol of gas from 1 atm (24.47 L mol^{-1}) to 1 M (1 mol L^{-1})) was made to the calculated solvation free energy, as discussed thoroughly by Jang et al.[30]

The calculated first two protonation constants for NTPA ligand using TC 1 and 2 are summarized in Table 2; results obtained are far from satisfactory (see δ, the difference between the computed and experimental values). In an attempt to improve the prediction of computed protonation constants, slightly modified procedure was employed. It involved full energy optimization of the ligand species in solvent (PCM/UA0) followed by single point calculations in the solvent (CPCM/UAHF) to generate ΔG_{sol}; similar approach[2] resulted in some improvement in computed dissociation constants. Data obtained here is included in Tables 1 and 2. From Table 2 it is seen that

TABLE 1: Selected Thermochemical Data (E_{min} = ZPVE-Corrected Energy) Obtained for Indicated NTPA Species, H_2O, and H_3O^+

	gas-phase optimized structures		SPC in solvent	solvent optimized structures	SPC in solvent
species	E_{min}[a]	G_{gas}[a]	ΔG_{sol}[b]	E_{min}[a]	ΔG_{sol}[b]
L^{3-}	−856.307384	−856.358126	−335.26	−856.825492	−338.92
HL^{2-}	−857.007834	−857.058753	−184.84	−857.290671	−191.7
H_2L^-	−857.615989	−857.664227	−71.96	−857.742252	−87.05
H_2O	−76.437174	−76.454816	−6.72	−76.452207	−6.9
H_3O^+	−76.696787	−76.714893	−107.35	−76.840274	−109.78

[a] In atomic unit, hartree (1 hartree = 627.5095 kcal/mol). [b] In kcal/mol.

TABLE 2: Comparison of Experimental and Calculated Protonation Constants, as log K_H, Using Gas-Phase and Solvent Optimized Structures Seen in Figure 2

		gas-phase structure				solvent structure			
reaction	exp[a]	TC 1	δ	TC 2	δ	TC 1	δ	TC 2	δ
$L^{3-} + H^+ = HL^{2-}$	9.49	12.06[b]	2.57	15.49[b]	6.00	14.40[b]	4.91	16.18[b]	6.69
		11.20[c]	1.71	30.13[c]	20.64	13.58[c]	4.09	31.67[c]	22.18
$HL^{2-} + H^+ = H_2L^-$	4.22	−4.19[b]	−8.41	−0.76[b]	−4.98	1.84[b]	−2.38	3.62[b]	−0.60

[a] Experimental protonation constants[4] at 20 °C and ionic strength = 0.1 M. [b] The CPCM-UAHF model was used for SPC. [c] The PCM-UA0 model was used for SPC.

(i) TC 1 worked better for the first protonation constant for both, gas-phase and solvent, structures, (ii) gas-optimized structures generated smaller errors in computed first protonation constant when compared with equivalent solvent structures values, and (iii) smaller errors in the second protonation constant were obtained from solvent structures, which is opposite to what is observed for the first protonation constant. Also the influence of the solvation model used at the SPC was tested; the use of PCM/UA0 somewhat improved the prediction generated from TC 1 and made them erroneous when TC 2 was employed. For some reasons, the simplified solvation model did not work at all for the second protonation reaction. There seems to be no obvious pattern in the data seen in Table 2 and, on average, results obtained are totally unacceptable due to large differences (δ) between the computed and experimental values. There are several possible sources for such large errors in computed values and some of them were discussed extensively elsewhere.[11,46] Regardless of the reasons applicable to this particular case, we came to the conclusion that because it is impossible to optimize all necessary protonated forms of the ligand NTPA in the gas phase, further investigations involving different levels of theory, larger basis sets, other solvation models, or different thermodynamic cycles were not, in our opinion, a justifiable option.

Isodesmic Reactions. Because we were not able to compute protonation constants with acceptable accuracy by employing TCs, we turned our attention to applicability of methodology based on isodesmic reaction (IRn). An IRn can be applied when the total number of each type of a bond is identical in the reactants and products.[63] To date, isodesmic reactions have been used to predict enthalpies of formation[69−77] and in some cases they have been incorporated within thermodynamic cycles to predict dissociation constants.[1,6−9] IRn is commonly used to investigate processes in a solvent (such as water) as it should minimize (or systematically cancel of) errors related to the solvation model used[51] (similar error should be introduced into each component within the reaction) provided that the same level of theory, basis set and solvation model is used for each component involved in the reaction. It can only be employed if accurate experimental energy/constant is available for the reference species used in the isodesmic reaction.[51,69] Interestingly, we have not found an explicit application of IRn in theoretical study of protonation/dissociation constants; for whatever reasons, which we do not understand fully, only different kinds of TC were employed till now and almost exclusively in case of monodissociable organic acids. We assumed that (i) weakness of presently available solvation models, particularly when poly negatively charged ions are investigated, is mainly responsible for large errors in protonation constants generated from TC-based computations and (ii) the use of isodesmic reaction methodology might eliminate to a significant degree errors typically associated with the use of TC.

The main challenge associated with the use of isodesmic reaction is the selection of the appropriate reference molecule. Taking into account structural properties of NTPA (called further $L_{(1)}$), we opted for NTA and IDA as reference compounds (called further $L_{(2)}$) because they have the same number (in case of NTA) and kind of electron donor atoms that can be protonated in a solution. Also, protonation constants of NTA and IDA are known as they are widely studied ligands.[4,5]

Isodesmic reaction can be seen here as simply a competition reaction between two ligands for a proton, and for the first protonation constant of NTPA it can be written as

$$L_{(1)}(aq) + HL_{(2)}(aq) = HL_{(1)}(aq) + L_{(2)}(aq) \qquad \Delta G_{aq} \tag{11}$$

Each of the two ligands (NTPA and reference molecule) is involved in several stepwise protonation reaction; for simplicity, only the first is shown

$$H^+ + L_{(1)} \leftrightarrow HL_{(1)} \qquad \Delta G_1(aq) = -\Delta G_{1d}(aq) \tag{12}$$

$$H^+ + L_{(2)} \leftrightarrow HL_{(2)} \qquad \Delta G_2(aq) = -\Delta G_{2d}(aq) \tag{13}$$

where $\Delta G_{nd}(aq)$ refers to reverse and relevant stepwise dissociation reaction. The change in Gibbs energies for each protonation reaction can be written as

$$\Delta G_1(aq) = G_{aq}(HL_{(1)}) - G_{aq}(H^+) - G_{aq}(L_{(1)}) \tag{14}$$

$$\Delta G_2(\mathrm{aq}) = G_{\mathrm{aq}}(\mathrm{HL}_{(2)}) - G_{\mathrm{aq}}(\mathrm{H}^+) - G_{\mathrm{aq}}(\mathrm{L}_{(2)}) \quad (15)$$

The isodesmic reaction of interest (eq 11) can be obtained by subtracting eq 13 from eq 12, and hence by subtracting eq 15 from eq 14, one obtains expression for the change in Gibbs energy, $\Delta G_{\mathrm{aq}} = \Delta G_1(\mathrm{aq}) - \Delta G_2(\mathrm{aq})$ applicable to this isodesmic reaction, where the uncertainty related to $G_{\mathrm{aq}}(\mathrm{H}^+)$ is no more applicable as this term cancels

$$\Delta G_{\mathrm{aq}} = \Delta G_1(\mathrm{aq}) - \Delta G_2(\mathrm{aq}) = G_{\mathrm{aq}}(\mathrm{HL}_{(1)}) - G_{\mathrm{aq}}(\mathrm{L}_{(1)}) - G_{\mathrm{aq}}(\mathrm{HL}_{(2)}) + G_{\mathrm{aq}}(\mathrm{L}_{(2)}) \quad (16)$$

Equation 16 was used to calculate ΔG_{aq} of isodesmic reaction (eq 11) from appropriate Gibbs energies obtained for relevant and fully solvent-optimized structures of the ligand NTPA and reference ligand $\mathrm{L}_{(2)}$. Table S2 in Supporting Information provides the ZPVE-corrected minimum energies E_{min} as well as Gibbs free energies for NTPA and IDA (energies of solvent-minimized structures of IDA and relevant data for the reference ligand NTA are shown in Figure S1 and Table S3, respectively, in Supporting Information). There are two energies listed for the H_3L form of the ligand NTPA, one of which refers to the optimized crystal structure H_3L^*; they were both utilized in the calculation of stepwise protonation constants of NTPA to determine which yielded better results, as these two structures have some distinguishable features.

The value of $\Delta G_2(\mathrm{aq})$ was obtained from eq 9 using reported protonation constants (at 25 °C and $\mu = 0.0$ and 0.1 M) of the $\mathrm{L}_{(2)}$ ligands, NTA and IDA. Having ΔG_{aq} and $\Delta G_2(\mathrm{aq})$, one can obtain $\Delta G_1(\mathrm{aq})$ (needed to calculate protonation constants of NTPA) from eq 16. Table 3 provides the values of functions required to calculate protonation constants, calculated and experimental protonation constants of the ligand NTPA, and the differences between calculated and experimental protonation constants (δ). For all isodesmic reactions seen in Table 3 the reference ligand is singly protonated; hence only the first protonation constant of IDA[4] was used to calculate $\Delta G_2(\mathrm{aq})$. Values obtained were −13.358 and −12.744 kcal mol^{-1} from experimental protonation constants ($\log K_{\mathrm{H}} = 9.79$ and 9.34) at ionic strengths 0.0 and 0.1 M, respectively, both at 25 °C.

A number of different isodesmic reactions have been tested, but only those that produced the best results have been reproduced in Table 3 (the remaining results, also involving NTA ligand, are provided in Table S4 of the Supporting Information). It is seen from Table 3 that application of isodesmic reactions resulted in much better overall prediction for the protonation constants when compared with results generated from TCs (Table 2). It is important to stress here that the available experimental protonation constants[4] of NTPA at $\mu = 0.1$ M and 20 °C (except for the forth one, $\mu = 0.5$ M and 25 °C) were compared against computed values generated with inclusion of protonation constants of the reference molecule IDA at $\mu = 0.0$ and 0.1 M, both at 25 °C. Paying attention to ionic strength at which experimental values were obtained was not common practice in the literature when TCs were employed but we worked on the assumption that, due to the inherent property of the isodesmic reaction, the prediction of the computationally generated protonation constant, if possible, must be at the same ionic strength as the experimental values used for the reference ligand. In other words, the values of $\Delta G_1(\mathrm{aq})$ (computed) and $\Delta G_2(\mathrm{aq})$ (experimental value of the reference molecule) should be at the same ionic strength because, by subtracting them, the influence of ionic strength should cancel out and the standard state function ΔG_{aq}, as computed for isodesmic reaction 11, is obtained.

From Table 3 it can also be seen that $K_{\mathrm{H}}^{(1)}$, $K_{\mathrm{H}}^{(2)}$, and $K_{\mathrm{H}}^{(4)}$ values, as log K_{H}, of NTPA (when protonation constants of IDA at ionic strength of 0.1 M were utilized) are predicted with excellent accuracy; the H_3L structure was employed in the case of the third and fourth protonation constants. Incorporating the H_3L^* structure resulted in excellent prediction of $K_{\mathrm{H}}^{(3)}$, the third protonation constant, but a rather poor result was obtained for $K_{\mathrm{H}}^{(4)}$. Interestingly, the δ values of poor predictions are almost identical, 2.66 and 2.76 log unit in the case of the self-constructed and crystallographic structure of H_3L used to calculate $K_{\mathrm{H}}^{(3)}$, and $K_{\mathrm{H}}^{(4)}$, respectively. This observation and analysis of results seen in Table 3 led us to the conclusion that the structural differences between self-constructed H_3L and crystallographic H_3L^* were responsible for the observed significant differences between experimental and computed protonation constants. If this were indeed the case, then one should perform full conformational analysis in a solvent of all possible protonated forms of molecules involved prior to application of isodesmic reaction. Interestingly, to the best of our knowledge, full conformational analysis was not utilized when dissociation constants were computed from TCs; this is a time-consuming exercise particularly when performed in Gaussian, and we embarked on that as a separate project to investigate the influence of small structural changes on the accuracy of computed protonation constants (results will be reported elsewhere), but at the same time decided to conduct here a simplified test. All forms of NTPA and IDA were subjected to the Schrödinger's Maestro[78] conformational analysis. This software automatically generates hundreds of possible conformers and estimates their energies in a short time based on MM/MD principles. It was of great interest to us to find out about predictions made by MM/MD analysis and whether this kind of conformational analysis would be of any use and help in this study. The structures of NTPA seen in Figure 2 were used as inputs for MM/MD conformational analysis in a solvent

TABLE 3: Comparison of Experimental[4] (Exp) at $\mu = 0.1$ M and 20 °C and Calculated Stepwise Protonation Constants of NTPA, as log K_{H}, Using First Protonation Constant of the Reference Molecule IDA at Ionic Strength $\mu = 0.0$ and 0.1 M and 25 °C (All Energies in kcal/mol)

		$\mu = 0.0$ M, 25 °C (IDA)				$\mu = 0.1$ M, 25 °C (IDA)			
reaction	ΔG_{aq}	$\Delta G_1(\mathrm{aq})$	log K_{H}	exp	δ	$\Delta G_1(\mathrm{aq})$	log K_{H}	exp	δ
$L_{(1)}^{3-} + HL_{(2)}^{-} = HL_{(1)}^{2-} + L_{(2)}^{2-}$	−1.223	−14.581	10.69	9.49	1.20	−13.967	10.24	9.49	0.75
$HL_{(1)}^{2-} + HL_{(2)}^{-} = H_2L_{(1)}^{-} + L_{(2)}^{2-}$	6.719	−6.639	4.87	4.22	0.65	−6.025	4.42	4.22	0.20
$H_2L_{(1)}^{-} + HL_{(2)}^{-} = H_3L_{(1)} + L_{(2)}^{2-}$	11.350	−2.008	1.47	3.68	−2.21	−1.394	1.02	3.68	−2.66
$H_3L_{(1)} + HL_{(2)}^{-} = H_4L_{(1)}^{+} + L_{(2)}^{2-}$	9.060	−4.298	3.15	2.71[a]	0.44	−3.684	2.70	2.71[a]	−0.01
$H_2L_{(1)}^{-} + HL_{(2)}^{-} = H_3L_{(1)}^{*} + L_{(2)}^{2-}$	7.602	−5.755	4.22	3.68	0.54	−5.141	3.77	3.68	0.09
$H_3L_{(1)}^{*} + HL_{(2)}^{-} = H_4L_{(1)}^{+} + L_{(2)}^{2-}$	12.807	−0.550	0.40	2.71[a]	−2.31	0.064	−0.05	2.71[a]	−2.76

[a] Experimental NTPA protonation constant[4] at $\mu = 0.5$ M and 25 °C.

TABLE 4: (a) Minimum Energies of MM/MD-Generated Conformers in Solvent (C1−C5) and Energies Obtained from MM-Based SPC Performed on the NTPA Structures Seen in Figure 2 and (b) Solvent-Optimized Energies of All Protonated Forms of the Ligand NTPA Obtained from DFT Calculations (E_{min} = ZPVE-Corrected Energy) of Structures Seen in Figure 2 and Lowest Energy MM/MD-Generated C1 Conformers

Part a[a]

L = NTPA	E_{SPC}	E_{C1}	δE (kJ/mol)	δE (kcal/mol)	C2	C3	C4	C5
L^{3-}	−947.64	−962.90	15.26	3.65	−962.89	−960.04	−960.04	−959.97
HL^{2-}	−1156.19	−1208.80	52.61	12.57	−1208.80	−1207.27	−1207.27	−1207.24
H_2L^-	−910.03	−957.14	47.11	11.26	−957.13	−956.01	−956.00	−955.67
H_3L	−615.06	−701.41	86.35	20.64	−701.19	−701.19	−700.21	−698.73
H_3L*	−658.92	−716.44	57.52	13.75	−715.10	−713.39	−713.26	−712.96
H_4L^+	−379.64	−435.17	55.53	13.27	−435.16	−433.09	−433.09	−430.78

Part b[b]

	Structures seen in Figure 2		C1			
L = NTPA	E_{min} (hartree)	G_{aq} (hartree)	E_{min} (hartree)	G_{aq} (hartree)	δG_{aq} (hartree)	δG_{aq} (kcal/mol)
L^{3-}	−856.825492	−856.875606	−856.828229	*−856.877193*	0.001587	1.00
HL^{2-}	−857.290671	−857.339621	−857.294193	*−857.342045*	0.002424	1.52
H_2L^-	−857.742252	−857.790980	−857.745414	*−857.792633*	0.001653	1.04
H_3L	−858.185011	−858.234959	−858.195297	*−858.241670*	0.006711	4.21
H_3L*	−858.192859	−858.240931	−858.184953	−858.229956	0.010975	6.89
H_4L^+	−858.633248	*−858.682587*	−858.635423	−858.681482	0.001105	0.69

[a] $\delta E = E_{SPC} - E_{C1}$. [b] $\delta G_{aq} = G_{aq}$(structure in Figure 2) − G_{aq}(C1).

TABLE 5: (a) Minimum Energies of MM/MD-Generated Conformers in Solvent (C1−C5) and Energies Obtained from MM-Based SPC Performed on the IDA Structures Seen in Figure S1 (*Supporting Information*) and (b) Solvent-Optimized Energies of All Protonated Forms of the Ligand IDA Obtained from DFT Calculations (E_{min} = ZPVE − Corrected Energy) of Structures Seen in Figure S1 (*Supporting Information*) and Lowest Energy MM/MD-Generated C1 Conformers

Part a[a]

L = IDA	E_{SPC}	E_{C1}	δE (kJ/mol)	δE (kcal/mol)	C2	C3	C4	C5
L^{2-}	−663.08	−676.62	13.53	3.23	−676.52	−676.52	−657.54	−657.53
HL^-	−1002.94	−1034.18	31.24	7.47	−1034.17	−1031.99		
H_2L	−759.59	−794.46	34.88	8.34	−794.46	−793.52	−793.51	−792.31
H_3L^+	−483.78	−517.66	33.88	8.10	−517.64	−517.38	−514.21	−514.20

Part b[b]

	Structures seen in Figure S1		C1			
L = IDA	E_{min} (hartree)	G_{aq} (hartree)	E_{min} (hartree)	G_{aq}(hartree)	δG_{aq} (hartree)	δG_{aq} (kcal/mol)
L^{2-}	−511.483326	*−511.519032*	−511.483246	−511.518986	−0.000046	−0.03
HL^-	−511.945458	−511.981098	−511.945929	*−511.982547*	0.001449	0.91
H_2L	−512.387398	*−512.423365*	−512.385598	−512.422578	−0.000787	−0.49
H_3L^+	−512.825900	*−512.862287*	−512.821788	−512.858264	−0.004023	−2.52

[a] $\delta E = E_{SPC} - E_{C1}$. [b] $\delta G_{aq} = G_{aq}$(structure in Figure S1) − G_{aq}(C1).

(generated structures of lowest energy are shown in Figure S2 in the Supporting Information). Table 4a provides energies (in kJ mol^{-1}) of the five lowest in energy MM/MD conformers (C1 to C5) of all protonated forms of NTPA seen in Figure 2. Also, SPC on the structures from Figure 2 was performed in solvent using MM to compare these energies with lowest energy MM/MD relevant conformer; obtained data are also included in Table 4a. It was of some concern to see that all the MM-generated structures were of considerably lower energy with the difference δ reaching over 20 kcal mol^{-1} (equivalent of about 14 log units in protonation constants) in the case of H_3L (a much lower difference was obtained for H_3L*). Because of that, the MM/MD-generated C1 conformers were fully solvent-optimized in Gaussian using the same procedure as described above for protonated NTPA species; results obtained are shown in Table 4b. It was gratifying to see that, even though all energies obtained from SPC (involving MM) were lower in value, the differences came down to a single kilocalorie range except H_3L and H_3L* for which δG = 4.21 and 6.89 kcal mol^{-1}, respectively. A similar procedure was applied to all the protonated forms of IDA, and results are shown in Table 5. All SPC-generated energies of IDA were again lower in value when compared with energies of the fully optimized structures seen in Figure 2 (Table 5a where $\delta E = E - E_{C1} > 0$). However, when C1 structures of IDA were fully DFT optimized, the resultant energies were lower in value when compared with the lowest energies of C1 conformers (see Table 5b where $\delta G < 0$ for all except HL) and it was gratifying to see that the δG values were rather small. From that, it might follow that to perform proper structural analysis in search of the lowest energy conformer, one would have to analyze a number of structures obtained from the MM/MD optimization. Our aim here was to prove the point that indeed it is possible to theoretically predict four consecutive protonation constants with acceptable accuracy (we were not interested in this work to find out how accurate that prediction might be); hence we did not proceed with full

TABLE 6: Comparison of Experimental[4] (Exp) at $\mu = 0.1$ M and 20 °C and Calculated Stepwise Protonation Constants of NTPA, as log K_H, Using the Lowest Energy Structures from Tables 4 and 5 (Seen in Italic) with Protonation Constants of the Reference Molecule IDA at Ionic Strength $\mu = 0.0$ and 0.1 M

	$\mu = 0.0$ M, 25 °C (IDA)			$\mu = 0.1$ M,25°C(IDA)		
reaction	log K_H	exp	δ	log K_H	exp	δ
$L_{(1)}^{3-} + HL_{(2)}^{-} = HL_{(1)}^{2-} + L_{(2)}^{2-}$	10.40	9.49	0.91	9.95	9.49	0.46
$HL_{(1)}^{2-} + HL_{(2)}^{-} = H_2L_1^{-} + L_{(2)}^{2-}$	3.84	4.22	−0.38	3.39	4.22	−0.83
$H_2L_{(1)}^{-} + HL_{(2)}^{-} = H_3L_{(1)} + L_{(2)}^{2-}$	3.13	3.68	−0.55	2.68	3.68	−1.00
$H_3L_{(1)} + H_2L_{(2)} = H_4L_{(1)}^{+} + HL_{(2)}^{-}$	2.89	2.71[a]	0.18	2.67	2.71[a]	−0.04

[a] Experimental NTPA protonation constant[4] at $\mu = 0.5$ M and 25 °C.

analysis of all the MM/MD-generated conformers. It appears, however, that MM/MD analysis might be a useful tool in search of conformers for the purpose of this kind of study.

We have selected from Tables 4 and 5 relevant NTPA and IDA structures that had the lowest DFT-computed G_{aq} (printed in italic in Tables 4 and 5) and used them for the protonation constants calculations based on the isodesmic reaction approach discussed earlier; results are shown in Table 6. The differences between experimental and computed values obtained at both ionic strengths are within ±1 log unit; this must be seen as an exceptional result because poly negatively charged structures were investigated here and similar in magnitude departures from experimental values were reported only for protonation constants of singly protonated common organic acids. An additional important fact is that the three experimental protonation constants (log $K_H^{(2)}$, log $K_H^{(3)}$, and log $K_H^{(4)}$) do not differ in value much (by less than a log unit) and computed values, even though with errors of the same dimension, they follow the experimental trend correctly, namely, log $K_H^{(2)}$ > log $K_H^{(3)}$ > log $K_H^{(4)}$. Comparison of data in Tables 3 and 6 supports the above supposition that accuracy in predicted (computed) protonation constants depends on conformational structure used for both molecules (the studied and reference one); it was possible to improve (on average) computed protonation constants by use of simplified, MM/MD conformational analysis.

It is important to realize that energy optimization operation of all molecules, even though performed in a solvent, most likely does not result in the exact molecular structure (and hence the computed minimum energy) as would exist in solution. This is most likely why exact (to the second decimal place) prediction of protonation constants is not possible when the described protocol is implemented. Nevertheless, results obtained are very encouraging and suitable for many applications, where the exact value might not be of absolute necessity. We came to the conclusion that implementation of isodesmic reaction methodology provides, or might provide, computed protonation constants at acceptable accuracy. This broadens, in our opinion, the scope of studying protonation constants computationally and opens a new field of applications for poly charged ligands.

Incorporation of IDA rather than NTA in isodesmic reaction has resulted in much better prediction of protonation constants. The reason for that is not clear at this stage, as one would expect that NTA, being structurally much closer to NTPA, should generate better results; work is in progress to explain this phenomenon. It is evident, however, that the selection of the reference molecule plays a crucial role and most likely it should be selected individually according to structural properties of a molecule under investigation. It is not surprising, then, that the use of acetic acid as a single reference molecule in the study of a large number and structurally different monoprotonated organic acids (and also without conformational analysis) often resulted in very large errors in the predicted dissociation constants.[1]

4. Conclusion

We have shown that prediction of several consecutive protonation constants for the highly and negatively charged molecules, such as NTPA, is possible with acceptable accuracy when isodesmic reaction methodology, instead of commonly employed thermodynamic cycle, is employed. Four stepwise protonation constants of NTPA were computed to within ±1 log unit of experimental data with an average error in the protonation constant of about 0.5 log unit. This good agreement was achieved for minimum energy structures of NTPA (studied ligand) and IDA (reference molecule) obtained from MM/MD conformational analysis followed by full energy optimization in solvent by Gaussian. It is reasonable to assume that even better estimates might be generated computationally when a number of lowest energy MM/MD-generated conformers were subjected to the DFT optimization in search for global minimum energy conformers. It appears that full conformational analysis should be seen as prerequisite for computing protonation/dissociation constants from IRn and possibly also from TC.

Results obtained in this study from TC agree with the literature reports in that TC methodology does not provide acceptably accurate results for poly negatively charged molecules. Also, we have demonstrated that in the gas phase the proton prefers to be bound to $-COO^-$ group (to form $-COOH$) rather than to nitrogen in NTPA; this severely restricts the use of TC in the study of numerous ligands.

Acknowledgment. Financial support of the National Research Foundation of South Africa and the University of Pretoria is highly appreciated.

Supporting Information Available: This consists of the tabulated (i) Comparison of experimental (CSD) and computed selected bond distances and angles for the H_3L^* and H_3L forms of NTPA, (ii) ZPVE-corrected minimum and Gibbs free energies of the NTA ligand obtained in solvent, (iii) ZPVE-corrected minimum and Gibbs free energies of the NTA ligand obtained in solvent, and (iv) comparison of experimental and numerous calculated from isodesmic reactions protonation constants of NTPA, as log K_H, using protonation constants of the reference molecules NTA and IDA at ionic strength $\mu = 0$ and 0.1 M. Figures show (i) solvent-optimized structures of IDA, and (ii) comparison of the DFT-generated structures of NTPA and lowest energy structures obtained from MM/MD-based conformational analysis performed on the DFT-optimized relevant structures. This material is available free of charge via the Internet at http://pubs.acs.org.

References and Notes

(1) Namazian, M.; Halvani, S. *J. Chem. Thermodyn.* **2006**, *38*, 1495.
(2) Saracino, G. A. A.; Improta, R.; Barone, V. *Chem. Phys. Lett.* **2003**, *373*, 411.

(3) Schuurmann, G.; Cossi, M.; Barone, V.; Tomasi, J. *J. Phys. Chem. A* **1998**, *102*, 6706.
(4) NIST Standard Reference Database 46. NIST Critically Selected Stability Constants of Metal Complexes Database, Version 8.0, Data collected and selected by R. M. Smith and A. E. Martell, U.S. Department of Commerce, National Institute of Standards and Technology, 2004.
(5) The IUPAC Stability Constants Database, http://www.iupac.org distributed and maintained by Academic Software, Sourby Old Farm, Timble, Otley, Yorks, LS21 2PW, U.K. (http://www.acadsoft.co.uk/scdbase/).
(6) Namazian, M.; Heidary, H. *J. Mol. Struct. (THEOCHEM)* **2003**, *620*, 257.
(7) Namazian, M.; Halvani, S.; Noorbala, M. R. *J. Mol. Struct. (THEOCHEM)* **2004**, *711*, 13.
(8) Namazian, M.; F.; Kalantary-Fotooh Noorbala, M. R.; Searles, D. J.; Coote, M. C. *J. Mol. Struct. (THEOCHEM)* **2006**, *758*, 275.
(9) Namazian, M.; Zakery, M.; Noorbala, M. R.; Coote, M. L. *Chem. Phys. Lett.* **2008**, *451*, 163.
(10) Charif, I. E.; Mekelleche, S. M.; Villemin, D.; Mora-Diez, N. *J. Mol. Struct. (THEOCHEM)* **2007**, *818*, 1.
(11) Liptak, M. D.; Shields, G. C. *Int. J. Quantum Chem.* **2001**, *85*, 727.
(12) Liptak, M. D.; Shields, G. C. *J. Am. Chem. Soc.* **2001**, *123*, 7314.
(13) Silva, C. O.; Silva, E. C.; Nascimento, M. A. C. *J. Phys. Chem. A* **2000**, *104*, 2402.
(14) Chipman, D. M. *J. Phys. Chem. A* **2002**, *106*, 7413.
(15) Klamt, A.; Eckert, F.; Diedenhofen, M.; Beck, M. E. *J. Phys. Chem. A* **2003**, *107*, 9380.
(16) Kelly, C. P.; Cramer, C. J.; Truhlar, D. G. *J. Phys. Chem. A* **2006**, *110*, 2493.
(17) Pliego, J. R., Jr.; Riveros, J. M. *J. Phys. Chem. A* **2002**, *106*, 7434.
(18) Klicic, J. J.; Friesner, R. A.; Liu, S.; Guida, W. C. *J. Phys. Chem. A* **2002**, *106*, 1327.
(19) Adam, K. R. *J. Phys. Chem. A* **2002**, *106*, 11963.
(20) Wiberg, K. B.; Clifford, S.; Jorgensen, W. L.; Frisch, M. J. *J. Phys. Chem. A* **2000**, *104*, 7625.
(21) Sang-Aroon, W.; Ruangpornvisuti, V. *Int. J. Quantum Chem.* **2008**, *108*, 1181.
(22) Bryantsev, V. S.; Diallo, M. S.; Goddard, W. A., III. *J. Phys. Chem. A* **2007**, *111*, 4422.
(23) Mujika, J. I.; Mercero, J. M.; Lopez, X. *J. Phys. Chem. A* **2003**, *107*, 6099.
(24) Gao, D.; Svoronos, P.; Wong, P. K.; Maddalena, D.; Hwang, J.; Walker, H. *J. Phys. Chem. A* **2005**, *109*, 10776.
(25) Li, H.; Hains, A. W.; Everts, J. E.; Robertson, A. D.; Jensen, J. H. *J. Phys. Chem. B* **2002**, *106*, 3486.
(26) Dahlke, E. E.; Cramer, C. J. *J. Phys. Org. Chem.* **2003**, *16*, 336.
(27) Liptak, M. D.; Gross, K. C.; Seybold, P. G.; Feldgus, S.; Shields, G. C. *J. Am. Chem. Soc.* **2002**, *124*, 6421.
(28) da Silva, G.; Kennedy, E. M.; Dlugogorski, B. Z. *J. Phys. Chem. A* **2006**, *110*, 11371.
(29) Silva, C. O.; Silva, E. C.; Nascimento, M. A. C. *Chem. Phys. Lett.* **2003**, *381*, 244.
(30) Ulander, J.; Broo, A. *Int. J. Quantum Chem.* **2005**, *105*, 866.
(31) Jang, Y. H.; Sowers, L. C.; Cagin, T.; Goddard, W. A., III. *J. Phys. Chem. A* **2001**, *105*, 274.
(32) Jang, Y. H.; Goddard, W. A., III; Noyes, K. T.; Sowers, L. C.; Hwang, S.; Chung, D. S. *J. Phys. Chem. B* **2003**, *107*, 344.
(33) Jitariu, L. C.; Masters, A. J.; Hiller, I. H. *J. Chem. Phys.* **2004**, *121*, 7795.
(34) Gross, K. C.; Seybold, P. G. *Int. J. Quantum Chem.* **2000**, *80*, 1107.
(35) Gross, K. C.; Seybold, P. G. *Int. J. Quantum Chem.* **2001**, *85*, 569.
(36) Byun, K.; Mo, Y.; Gao, J. *J. Am. Chem. Soc.* **2001**, *123*, 3974.
(37) Murlowska, K.; Sadlej-Sosnowska, N. *J. Phys. Chem. A* **2005**, *109*, 5590.
(38) Li, G.; Cui, Q. *J. Phys. Chem. B* **2003**, *107*, 14521.
(39) Himo, F.; Noodleman, L.; Blomberg, M. R. A.; Siegbahn, P. E. M. *J. Phys. Chem. A* **2002**, *106*, 8757.
(40) Magill, A. M.; Cavell, K. J.; Yates, B. F. *J. Am. Chem. Soc.* **2003**, *126*, 8717.
(41) Topol, I. A.; Burt, S. K.; Rashin, A. A.; Erickson, J. W. *J. Phys. Chem. A* **2000**, *104*, 866.
(42) Scharnagl, C.; Raupp-Kossmann, R. A. *J. Phys. Chem. B* **2004**, *108*, 477.
(43) Lee, I.; Kim, C. K.; Lee, I. Y.; Kim, C. K. *J. Phys. Chem. A* **2000**, *104*, 6332.
(44) Kubicki, J. D. *J. Phys. Chem. A* **2001**, *105*, 8756.
(45) Maksic, Z. B.; Vianello, R. *J. Phys. Chem. A* **2002**, *106*, 419.
(46) Davies, J. E.; Doltsinis, N. L.; Kirby, A. J.; Roussev, C. D.; Sprik, M. *J. Am. Chem. Soc.* **2002**, *124*, 6594.
(47) Kim, Y. J.; Streitwieser, A. *J. Am. Chem. Soc.* **2002**, *124*, 5757.
(48) Sadlej-Sosnowska, N. *Theor. Chem. Acc.* **2007**, *118*, 281.
(49) Merrill, G. N.; Fletcher, G. D. *J. Mol. Struct. (THEOCHEM)* **2008**, *849*, 84.
(50) Soriano, E.; Cerdan, S.; Ballesteros, P. *J. Mol. Struct. (THEOCHEM)* **2004**, *684*, 121.
(51) Cramer, C. J. *in Essentials of Computational Chemistry*; John Wiley & Sons Ltd.: New York, 2002.
(52) Barone, V.; Cossi, M. *J. Phys. Chem. A* **1998**, *102*, 1995.
(53) Montgomery, J. A.; Frisch, M. J.; Ochterski, J. W.; Petersson, G. A. *J. Chem. Phys.* **1999**, *110*, 2822.
(54) Ochterski, J. W.; Petersson, G. A.; Montgomery, J. A., Jr. *J. Chem. Phys.* **1996**, *104*, 2598.
(55) Petersson, G. A.; Malick, D. K.; Wilson, W. G.; Ochterski, J. W.; Montgomery, J. A.; Frisch, M. J. *J. Chem. Phys.* **1998**, *109*, 10570.
(56) Topol, I. A.; Tawa, G. J.; Burt, S. K.; Rashin, A. A. *J. Chem. Phys.* **1999**, *111*, 10998.
(57) Varadwaj, P. R.; Cukrowski, I.; Marques, H. M. *J. Phys. Chem. A* **2008**, *112*, 10657.
(58) Frisch, M. J; Trucks, G. W.; Schlegel, H. B.; Scuseria, G. E.; Robb, M. A.; Cheeseman, J. R.; Montgomery Jr., J. A.; Vreven, T.; Kudin, K. N.; Burant, J. C.; Millam, J. M.; Iyengar, S. S.; Tomasi, J.; Barone, V.; Mennucci, B.; Cossi, M.; Scalmani, G.; Rega, N.; Petersson, G. A.; Nakatsuji, H.; Hada, M.; Ehara, M.; Toyota, K.; Fukuda, R.; Hasegawa, J.; Ishida, M.; Nakajima, T.; Honda, Y.; Kitao, O.; Nakai, H.; Klene, M.; Li, X.; Knox, J. E.; Hratchian, H. P.; Cross, J. B.; Bakken, V.; Adamo, C.; Jaramillo, J.; Gomperts, R.; Stratmann, R. E.; Yazyev, O.; Austin, A. J.; Cammi, R.; Pomelli, C.; Ochterski, J. W.; Ayala, P. Y.; Morokuma, K.; Voth, G. A. , Salvador, P.; Dannenberg, J. J; Zakrzewski, V. G.; Dapprich, S.; Daniels, A. D.; Strain, M. C.; Farkas, O.; Malick, D. K.; Rabuck, A. D.; Raghavachari, K.; Foresman, J. B.; Ortiz, J. V.; Cui, Q.; Baboul, G.; Clifford, S.; Cioslowski, J.; Stefanov, B. B.; Liu, G.; Liashenko, A.; Piskorz, P.; Komaromi, I.; Martin, R. L.; Fox, D. J.; Keith, T.; Al-Laham, M. A.; Peng, C. Y.; Nanayakkara, A.; Challacombe, M.; Gill, P. M. W.; Johnson, B.; Chen, W.; Wong, M. W.; Gonzalez, C.; Pople, J. A. *Gaussian 03*, revision D.01, Gaussian, Inc.: Wallingford, CT, 2004.
(59) Stephens, P. J.; Devlin, F. J.; Chabalowski, C. F.; Frisch, M. J. *J. Phys. Chem.* **1994**, *98*, 11623.
(60) Cances, E.; Mennucci, B.; Tomasi, J. *J. Chem. Phys.* **1997**, *107*, 3032.
(61) Cossi, M.; Barone, V.; Cammi, R.; Tomasi, J. *Chem. Phys. Lett.* **1996**, *255*, 327.
(62) Miertus, S.; Scrocco, E.; Tomasi, J. *J. Chem. Phys.* **1981**, *55*, 117.
(63) Foresman, J. B.; Frisch, A. In *Exploring Chemistry with Electronic Structure Methods*; Gaussian, Inc.: Pittsburgh, PA, 1996.
(64) Cossi, M.; Rega, N.; Scalmani, G.; Barone, V. *J. Comput. Chem.* **2003**, *24*, 669.
(65) Walker, E. H., Jr.; Apblett, A. W.; Walker, R.; Zachary, A. *Chem. Mater.* **2004**, *16*, 5336.
(66) Allen, F. H. *Acta Crystallogr.* **2002**, *B58*, 380.
(67) Sang-Aroon, W.; Ruangpornvisuti, V. *J. Mol. Struct. (THEOCHEM)* **2006**, *758*, 181.
(68) Pliego, J. R., Jr. *Chem. Phys. Lett.* **2003**, *367*, 145.
(69) da Silva, G.; Bozzelli, J. W. *J. Phys. Chem. C* **2007**, *111*, 5760.
(70) da Silva, G.; Bozzelli, J. W. *J. Phys. Chem. A* **2006**, *110*, 13058.
(71) Guo, Y.; Gao, H.; Twamley, B.; Shreeve, J. M. *Adv. Mater.* **2007**, *19*, 2884.
(72) Espinosa-Garcia, J.; Garcia-Bernaldez, J. C. *Phys. Chem. Chem. Phys.* **2002**, *4*, 4096.
(73) Krossing, I.; Raabe, I. *Chem.−Eur. J.* **2004**, *10*, 5017.
(74) Kutt, A.; Movchun, V.; Rodima, T.; Dansauer, T.; Rusanov, E. B.; Leito, I.; Kaljurand, I.; Koppel, J.; Pihl, V.; Koppel, I.; Ovsjannikov, G.; Toom, L.; Mishima, M.; Medebielle, M.; Lork, E.; Roschenthaler, G.-V.; Koppel, I. A.; Kolomeitsev, A. A. *J. Org. Chem.* **2008**, *73*, 2607.
(75) Nolan, E. M.; Linck, R. G. *J. Am. Chem. Soc.* **2000**, *122*, 11497.
(76) Peeters, D.; Leroy, G.; Wilante, C. *J. Mol. Struct.* **1997**, *416*, 21.
(77) Wang, L.; Heard, D. E.; Pilling, M. J.; Seakins, P. *J. Phys. Chem. A* **2008**, *112*, 1832.
(78) Schrödinger Maestro, 32nd Floor, Tower 45, 120 West Forty-Fifth Street, New York, 10036.

JP811044B